LBL-1675

CONf-730117--3

RECEIVED BY TIC MAY 9 1973

21,273

MÖSSBAUER ISOMER SHIFTS OF THE 6.2-keV GAMMA RAYS OF TANTALUM-181

G. Kaindl, D. Salomon, and G. Wortmann

April 1973

LBL-1675

MASTER

DISCLAIMER

This report was prepared as an account of work sponsored by an agency of the United States Government. Neither the United States Government nor any agency thereof, nor any of their employees, makes any warranty, express or implied, or assumes any legal liability or responsibility for the accuracy, completeness, or usefulness of any information, apparatus, product, or process disclosed, or represents that its use would not infringe privately owned rights. Reference herein to any specific commercial product, process, or service by trade name, trademark, manufacturer, or otherwise does not necessarily constitute or imply its endorsement, recommendation, or favoring by the United States Government or any agency thereof. The views and opinions of authors expressed herein do not necessarily state or reflect those of the United States Government or any agency thereof.

DISCLAIMER

Portions of this document may be illegible in electronic image products. Images are produced from the best available original document.

Invited Talk Presented at

the Eighth Symposium on Mössbauer Effect Methodology,
New York City (1973).

LBL-1675

-1-

MÖSSBAUER ISOMER SHIFTS OF THE 6.2-keV GAMMA RAYS OF TANTALUM-181.

G. Kaindl

Lawrence Berkeley Laboratory, University of Cali-
fornia and Physik-Department, Technische Univer-
sität München.

D. Salomon

Lawrence Berkeley Laboratory, University of Ca-
lifornia.

G. Wortmann

Physik-Department, Technische Universität München.

I. INTRODUCTION

In attempting to improve the resolution of
the Mössbauer method considerable attention has
been devoted to the few potential Mössbauer reso-
nances with lifetimes in the microsecond region
[1-4]. It has been shown recently, that in particu-
lar the 6.2-keV gamma transition of Ta-181 ($T_{1/2}$ =
6.8 μs) warrants great promise for high-resolution
Mössbauer studies of hyperfine interactions. This
is true for magnetic-dipole and electric-quadru-
pole hyperfine interactions as well as for isomer
shifts [5-12].

Striking results have been obtained with iso-
mer shifts [5,12], which were found to cover a
total range of 110 mm/s. In view of the natural
width of the 6.2-keV gamma rays, $W_0 = 2\hbar/\tau = 0.0064$ mm/s,

and the presently best experimental linewidth, W_{exp}=0.069 mm/s [11] , this represents an improvement of the resolution in Mössbauer isomer shift studies by more than an order of magnitude. This resolution is due to three favorable properties of the 6.2-keV gamma resonance: the small natural width of the Mössbauer gamma rays, the high atomic number of tantalum, and the large magnitude of the change of the mean-squared nuclear charge radius ($\Delta<r^2>$) between the excited state and the ground state of tantalum-181.

The present paper consists of two main parts. In the first part (Sections II and III) the more general aspects of Ta-181 isomer shifts will be covered, including an estimate for $\Delta<r^2>$. The second part (Section IV) is devoted to solid-state applications, as exemplified by the study of the dependence of the transition energy of the 6.2-keV gamma rays on temperature and hydrostatic pressure.

II. EXPERIMENTAL TECHNIQUE

Isomer shifts of the 6.2-keV gamma rays of Ta-181 can be studied with standard Mössbauer technique. Due to the large potential lineshift/linewidth ratios, attention must, however, be given to the stability of the employed velocity drive, and an increased number of channels (up to 2000) should be available. In addition small solid angles ought to be used in order to prevent excessive geometrical broadening. For the present work a sinusoidal electromechanical velocity drive was used, and the data were evaluated in a way as described in Ref.13.

The main experimental difficulty with the 6.2-keV gamma resonance arises from the extreme sensitivity of hyperfine interactions to crystal inhomogeneities. This requires special care in the preparation of sources and absorbers. In the present work sources were prepared by diffusing W-181 activity into high-purity , and if available, single-crystal transition metals.W-181 of high specific activity was produced by activation of 93% enriched W-180 metal in integrated thermal neutron fluxes

ranging from 10^{21} to 10^{22} n/cm^2. The metal samples (about 1 mm thick and typically 6 mm diameter) were spark-cut from bulk materials and polished by the usual metallographic methods, including electro-polishing. W-181 activity was dropped onto the metal discs in form of an HF/HNO$_3$ solution and dried. Prior to diffusion in high vacuum (at 10^{-8} to 10^{-9} Torr) the tungsten activity was reduced in hydrogen atmosphere at 950° C for ~ 1/2 hour. (This hydrogen-reduction process was not performed with the palladium source). As a rule diffusion was performed at temperatures close to the melting points of the host metals. In case of the hafnium metal host, however, the diffusion temperature was kept below the hexagonal-cubic transition point at 1740° C. Some of the sources were also produced by resistance heating, but the method of induction heating was found more appropriate for the present purpose.

Absorbers were prepared from tantalum metal and from several tantalum compounds. The metal absorber was prepared from a tantalum metal foil of 99.996% nominal purity by a high-vacuum annealing and degassing procedure [4] . The foil was intermittently rolled between high-purity tantalum metal foils and annealed at 2300° C in a vacuum of ~ 10^{-9} Torr. Absorbers of TaC, KTaO$_3$, NaTaO$_3$, and LiTaO$_3$ were prepared by sedimentation in a polystyrene-benzene solution on a 6μ-thick mylar foil. During drying, a thin polystyrene film, containing the tantalum-compound in a relatively homogeneous layer, formed on the mylar.

III. GENERAL ASPECTS OF Ta-181 ISOMER SHIFTS

A. High-Resolution Isomer Shift Results

Isomer shifts were derived from source and absorber experiments, using a single-line Ta metal absorber and a single-line W-181(W) source, respectively. In both cases the isomer shifts will be reported relative to tantalum metal, with a sign convention where a more positive isomer shift corresponds to a larger transtion energy.

Some representative single-line spectra for metallic sources are shown in Fig. 1. The spectrum for the nickel host was obtained with the source heated above the Curie point of nickel metal, while in all other cases both source and absorber were kept at room temperature.
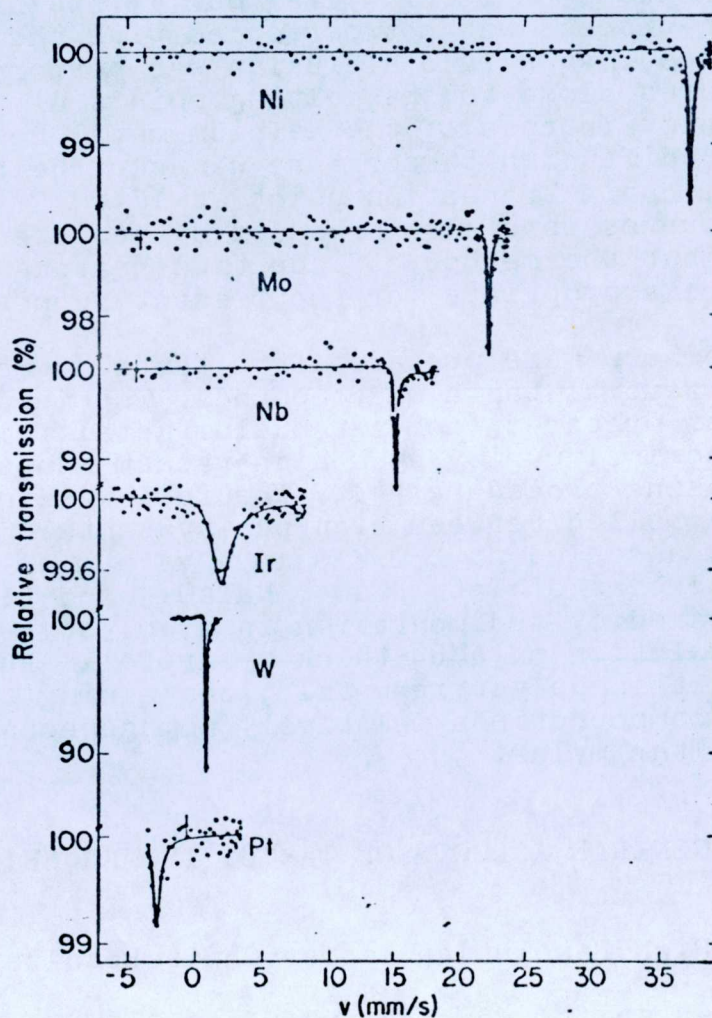

Fig. 1. Mössbauer absorption spectra of the 6.2-keV gamma rays for sources of W-181 diffused into various cubic transition-metal hosts.

The pronounced asymmetry in the lineshapes re-
sults from an interference between photoelectric
absorption and Mössbauer absorption followed by
internal conversion [16,17] . This effect, which
was originally observed by Sauer et al. [3] , is
particularly large for the 6.2-keV gamma rays due
to their E1 multipolarity, their low transition
energy, and their large internal-conversion coeffi-
cient. The absorption spectra were least-squares
fitted with dispersion-modified Lorentzian lines
of the form [16]

$$N(v) = N(\infty) - A(1 - 2\xi X)/(1 + X^2) \qquad (1)$$

with $X = 2(v-v_o)/W$. Here $N(v)$ is the intensity trans-
mitted at relative velocity v, v_o is the position
of the line, W is the full linewidth at half-ma-
ximum, and A is the amplitude of the line. The pa-
rameter ξ determines the relative magnitude of the
dispersion term. It has been shown previously
[5,18] that the experimental result, $2\xi = -0.31 + 0.01$,
agrees well with the theoretical prediction of
Ref. 16 . In the present work all spectra were fit-
ted with a constant amplitude of the dispersion
term, $2\xi = -0.31$.

Fig. 2 shows the absorption spectra measured
for sources of W-181 diffused into the hexagonal
metals rhenium, osmium, and ruthenium. In these
cases the emission spectra are split by electric-
quadrupole interactions [8,9] . In an axially-sym-
metric electric field gradient the $9/2^- \rightarrow 7/2^+$ E1
transition splits into 11 hyperfine components.
While the spectrum for osmium was obtained with a
polycrystalline source, both the rhenium and ruthen-
ium spectra were measured with single-crystal sour-
ces with the direction of observation perpendicular
to the [0001] -axis. The solid lines in Fig. 2 are
the results of least-squares fits of superpositions
of dispersion modified Lorentzian lines to the data.
In the fit procedures both the amplitude of the dis-
persion term, $2\xi = -0.31$, and the ratio of electric
quadrupole moments, $Q(9/2)/Q(7/2) = 1.133$ [8] , were
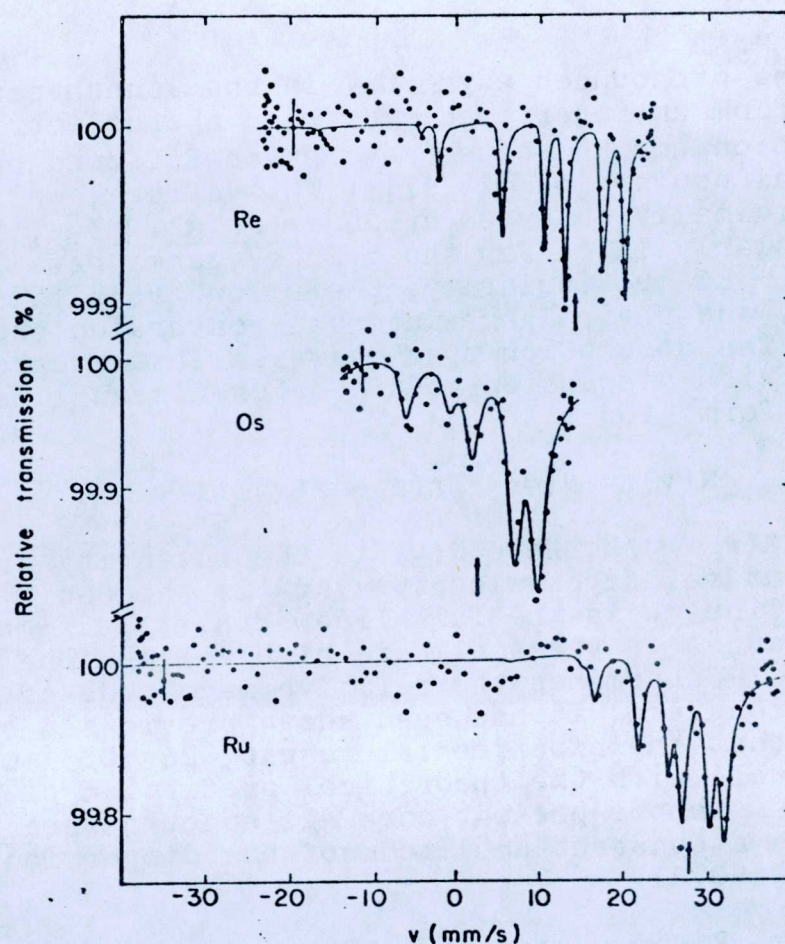kept constant.

Fig. 2. Electric-quadrupole split absorption spectra for sources of W-181 diffused into hexagonal transition metals. The centers of the absorption patterns are indicated by arrows.

Up to now Mössbauer absorption spectra of tantalum compounds have been observed only for a few pentavalent alkali tantalates and for TaC. The results for the tantalates are presented in Fig. 3. For $KTaO_3$, which has the cubic NaCl structure, a broadened single line was observed, while electric-quadrupole split spectra were found for hexagonal $LiTaO_3$ and orthorhombic $NaTaO_3$. The split spectra were least-squares fitted in an identical manner as those for the hexagonal host metals of

Fig. 2, assuming an axially-symmetric electric field gradient in both cases. In this way values for the isomer shifts, as well as for the signs and magnitudes of the electric field gradients at the tantalum sites, were obtained [10].
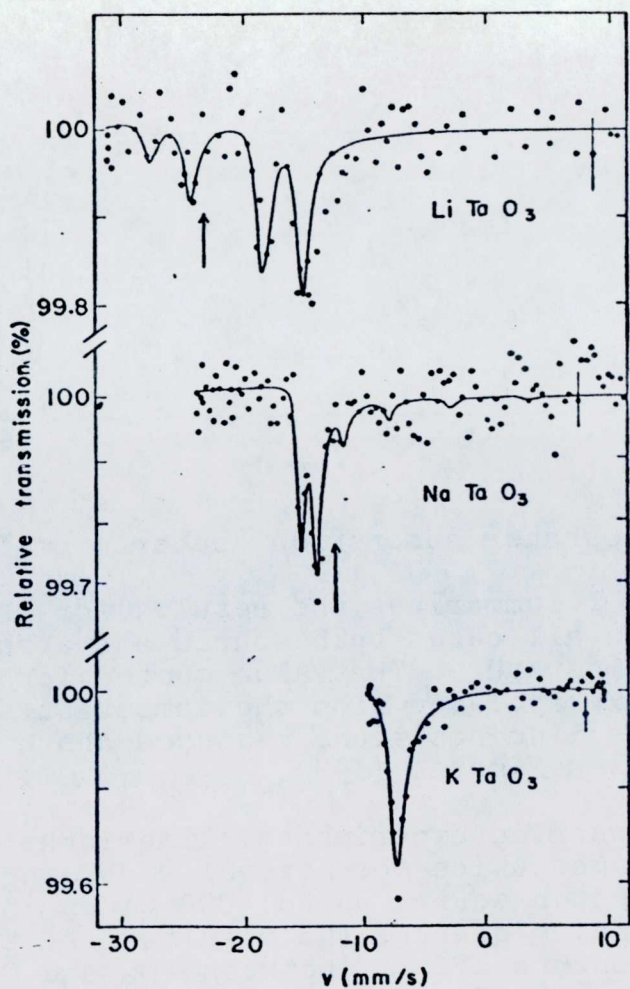

XBL728-3915.

Fig. 3. Mössbauer absorption spectra of alkali tantalates. The centers of the spectra are indicated by arrows.

Figure 4 shows the absorption spectrum of TaC. As expected from the cubic structure of TaC, a single, though broadened line was observed. This spectrum exhibits the largest isomer shift so far observed.
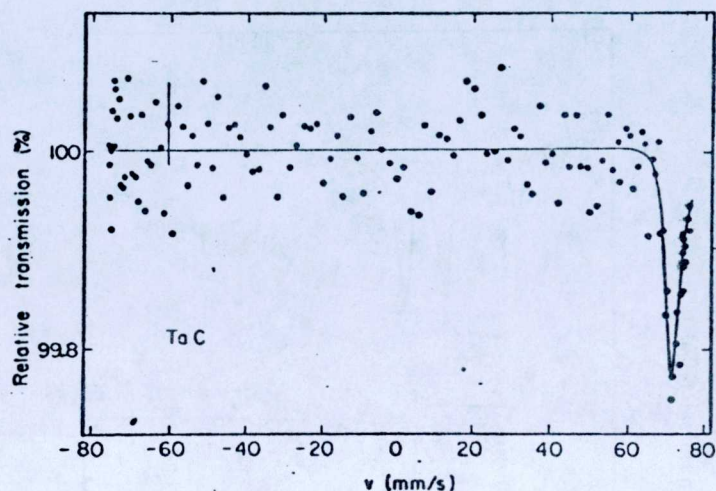

Fig. 4. Mössbauer absorption spectrum of TaC.

Table 1 summarizes the results for the isomer shift S. In all cases both source and absorber were at room temperature. The value quoted for the nickel host was extrapolated from the temperature dependence of the line position, measured above the Curie point of nickel metal [19] .

The observed experimental linewidths W range from ~11 times twice the natural width in the case of the tungsten source up to ~800 times in the case of the vanadium source. The magnitude of the observed resonance effect (between 20% and 0.2%) is strongly correlated with the experimental linewidth. The largest lineshift/linewidth ratios were found for the Mo, Nb, and Ni hosts, even though the experimental linewidths for these sources range from 20 to 77 times the theoretical minimum.

Results similar to ours were obtained by other groups only for the tungsten and tantalum hosts

[2-4,20] , and their data agree well with the present results.

Table 1. Summary of isomer shift results.

Source Lattice	S (mm/s)	W(FWHM) (mm/s)	Effect (%)
V	−33.2 (5)	5.0 (10)	0.1
Ni	−39.5 (2)	0.50 (8)	1.6
Nb	−15.26 (10)	0.19 (6)	1.5
Mo	−22.60 (10)	0.13 (4)	3.0
Ru	−27.50 (30)	1.3 (2)	0.7
Rh	−28.80 (25)	3.4 (5)	0.3
Pd	−27.80 (25)	1.3 (3)	0.3
Hf	−0.60 (30)	1.6 (4)	0.2
Ta	−0.075 (4)	0.184 (6)	2.4
W	−0.860 (8)	0.069 (1)	20
Re	−14.00 (10)	0.60 (4)	1.3
Os	−2.35 (4)	1.8 (2)	0.8
Ir	−1.84 (4)	1.60 (14)	0.5
Pt	+2.66 (4)	0.30 (8)	1.5
Absorber Lattice			
$LiTaO_3$	−24.04 (30)	1.6 (2)	0.9
$NaTaO_3$	−13.26 (30)	1.0 (2)	0.9
$KTaO_3$	− 8.11 (15)	1.5 (2)	0.3
TaC	+70.8 (5)	2.4 (4)	0.2

B. Systematics of Isomer Shifts for Ta-181 Impurities in Transition Metal Hosts.

The isomer shifts for dilute impurities of Ta-181 in transition-metal hosts exhibit systematic features when plotted versus the number of electrons in the valence shells of the various host

elements, as shown in Fig. 5. The data can be
arranged in three groups corresponding to 3d, 4d,
and 5d host metals. Without exception, the transi-
tion energy decreases from a 5d to a 4d and further
to a 3d host metal within the same column of the
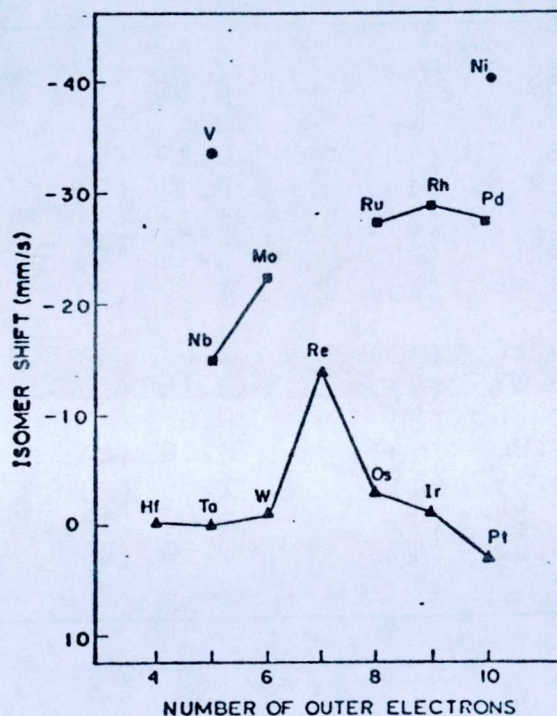periodic table.

Fig. 5. Systematics of isomer shifts of the 6.2-
keV gamma rays of Ta-181.

A similar systematic behaviour of isomer shifts
has been observed with gamma resonances of Fe-57
(14.4 keV) [21-24] , Ru-99(90 keV), Au-197(77 keV),
and Ir-193(73 keV)[15,25-27]. In all of these cases
estimates for the changes of the mean-squared nuc-
lear charge radii $\Delta<r^2>$ are reasonably well estab-
lished [28] , so that information on the systematic
behaviour of absolute electron densities at impurity

nuclei $(|\psi_o|^2)$ may be derived from these data. This in turn can be used to derive an estimate for $\Delta<r^2>$ of the present gamma resonance.
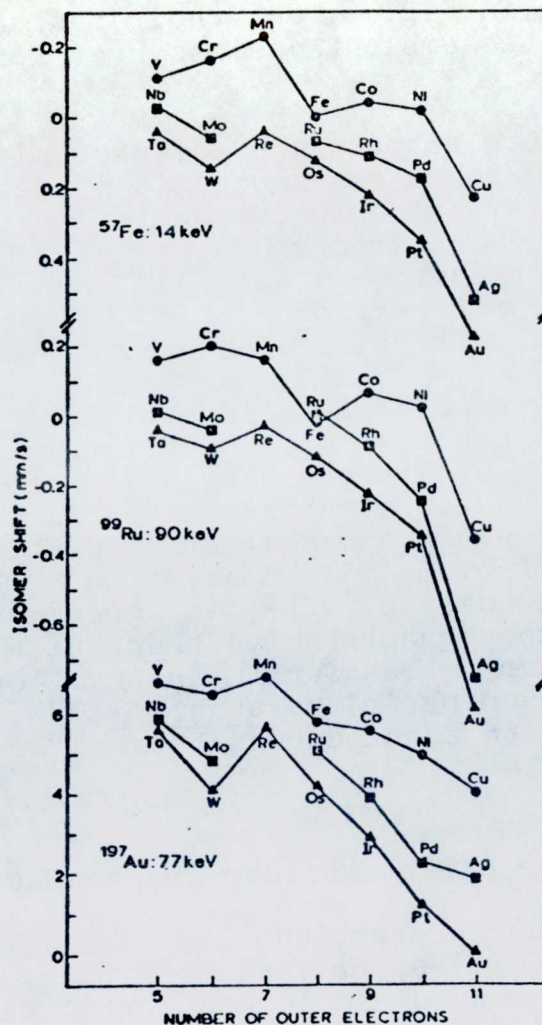

Fig. 6. Systematics of isomer shifts for dilute impurities of Fe-57, Ru-99, and Au-197, measured with gamma resonances of the impurity atoms at 14.4 keV, 90 keV, and 77 keV, respectively.

The isomer-shift data for impurities of Fe-57, Ru-99, and Au-197, measured with the relevant gamma resonances, are summarized in Fig. 6. The respective results for Ir-193 impurities [27] have not been included in Fig. 6, but their systematic features closely resemble those observed for impurities of Ru-99.

Taking into account the accepted signs of $\Delta <r^2>$ for the gamma resonances it is realized that $|\psi_0|^2$ at the various impurity nuclei increases from 5d via 4d to 3d homologous host metals. The only exceptions to this rule are found for hosts of iron and its d-electron homologues. In this column, however, the lattice structure changes from bcc to hcp.

Such a systematic behaviour of $|\psi_0|^2$ at the impurity atoms has been discussed theoretically by daSilva et al. [29] in connection with the Fe-57 data, using a pseudopotential approach. They predicted a decrease in the d-electron density at the impurity atom from 5d via 4d to 3d host metals, causing an increase in $|\psi_0|^2$, in agreement with observation. A more quantitative theoretical description of the charge transfer in Au-Ag alloys has recently been given by Gelatt et al. [30], taking into account both s and d charge transfer between the constituents.

C. Change of the Nuclear Charge Radius

A remarkable proportionality of differences of electron densities for various impurity atoms between homologous 5d and 4d host metal pairs is revealed if one forms ratios of isomer-shift differences. This is demonstrated in Table 2, where the ratios of the isomer shift differences observed with the Ta-181 gamma resonance to those observed with gamma resonances of Au-197, Ir-193, Ru-99, and Fe-57 are summarized. With only a few exceptions these ratios are quite constant within the limits of error for a given pair of gamma resonances.

Table 2. Ratios of isomer shift differences bet-
ween homologous 4d and 5d transition metal hosts
for the Ta-181 gamma resonance to those of gamma
resonances of Au-197 (77 keV), Ir-193 (73 keV),
Ru-99 (90 keV), and Fe-57 (14.4 keV).

X	$\Delta S(^{181}Ta)/ \Delta S(X)$				
	Nb-Ta	Mo-W	Ru-Os	Rh-Ir	Pd-Pt
^{197}Au	-54(6)	-29(2)	-28(2)	-27(2)	-29(2)
^{193}Ir	-57(10)	-59(14)	-58(3)	-44(2)	-47(3)
^{99}Ru	-276(57)	-235(27)	-231(14)	-223(19)	-248(31)
^{57}Fe	253(84)	240(27)	419(140)	245(22)	179(10)

The ratio of the changes of the mean-squared
nuclear charge radii $\Delta <r^2>$ of two different gamma
resonances is related to the ratio of isomer shift
differences ΔS by

$$\frac{\Delta <r^2>_1}{\Delta <r^2>_2} = \frac{E_1}{E_2} \frac{Z_2}{Z_1} \frac{\Delta S_1}{\Delta S_2} \frac{\Delta |\psi_o|^2_2}{\Delta |\psi_o|^2_1} \qquad (2)$$

Here the indices 1 and 2 refer to two separate gam-
ma resonances with energies E1 and E2 in elements
with atomic numbers Z_1 and Z_2, respectively. The
isomer shifts are measured in velocity units.
$\Delta |\psi_o|^2_2 / \Delta |\psi_o|^2_1$ stands for the ratio of electron den-
sity differences at the two nuclei for the same
pair of host lattices.

Thus to evaluate $\Delta <r^2>$ from Table 2, one has
to obtain information on the ratios of $\Delta |\psi_o|^2$ bet-
ween homologous 5d and 4d transition metal hosts for
the various impurity elements. It has been shown re-

cently [12] that these ratios can be obtained from
a comparison of isomer shifts in 5d and 4d transi-
tion metal hosts with those of isoelectronic com-
pounds of the two elements under discussion. This
is possible, since ratios of $\Delta|\psi_o|^2$ between iso-
electronic configurations of two elements can di-
rectly be derived from the results of free-ion self-
consistent field (SCF) calculations [31] . In the
cases of Ir-193, Ru-99, and Fe-57 enough isomer
shift data are available to allow an application of
this concept [32] . Unfortunately, this is not the
case with Ta-181. However, it has been shown
[12] that the ratios of $\Delta|\psi_o|^2$ between homologous
5d and 4d host metals for impurity elements of Ir-
193, Ru-99, and Fe-57, obtained in this way are not
drastically different from those derived directly
from SCF calculations with the assumption that the
magnitudes of the effective d → s charge transfer
occuring at the various impurity atoms, when trans-
ferring them from a 5d to the homologous 4d host,
are approximately equal: e.g. the differences were
found to be less than 30% for Ir, Ru, and Fe. Lack-
ing better knowledge we therefore assume approxi-
mately constant d → s charge transfer for impurity
atoms of Ta, Ir, and Au.

The ratios of $\Delta|\psi_o|^2$, given in Table 3 (col-
umn 3) were obtained with this assumption, using the
ratios of $\Delta|\psi_o|^2$ for impurity atoms of Ir-193 to
those of Ru-99 and Fe-57, as derived in Ref. 12 .
In the derivation of these ratios the results of
free-ion relativistic Dirac-Fock calculations for
Ru, Ta, and Au [33] and those of non-relativistic
Hartree-Fock calculations for Fe [34] and Ir [35]
were employed. In column 2 of Table 3 the weighted
mean values of the individual ratios of isomer
shift differences of Table 2 are listed. The de-
rived ratios of $\Delta<r^2>$ are then presented in column
4. With the $\Delta<r^2>$ values for the gamma resonances
of Au-197, Ir-193, Ru-99, and Fe-57 (column 5),
taken from Ref. 36, 28, 37, and 38, respectively,
the four estimates for $\Delta<r^2>$ of the 6.2-keV gamma
transition were obtained (column 6). As a final
result for $\Delta<r^2>$ we take the mean value of the
four estimates

$$\Delta<r^2> \quad = -5 \cdot 10^{-2} \qquad fm^2$$

Table 3. Derivation of $\Delta\langle r^2\rangle$ for the 6.2-keV gamma resonance from systematics of isomer shifts in transition metal hosts.

X	$\dfrac{\Delta S(^{181}Ta)}{\Delta S(X)}$	$\dfrac{\Delta\lvert\psi_o\rvert^2_{Ta}}{\Delta\lvert\psi_o\rvert^2_X}$	$\dfrac{\Delta\langle r^2\rangle_{Ta}}{\Delta\langle r^2\rangle_X}$	$\Delta\langle r^2\rangle_X$ $(10^{-3}\ fm^2)$	$\Delta\langle r^2\rangle_{Ta}$ $(10^{-3}\ fm^2)$
^{197}Au	−30	0.50	−5.2	9	−47
^{193}Ir	−49	0.69	−6.4	4.6	−29
^{99}Ru	−236	5.9	−1.7	25	−43
^{57}Fe	218	11.5	2.9	−25	−72
				average	−48

The uncertainty of this value can only be estimated, especially since it is directly correlated with the uncertainties in the $\Delta \langle r^2 \rangle$ values from which it was derived. We think, however, that 50% is an upper limit to the possible error. The result for $\Delta \langle r^2 \rangle$ of the 6.2-keV gamma transition represents one of the largest changes in nuclear charge radius observed up to now for Mössbauer transitions [28]. It is associated with a single-particle proton transition between the $9/2^-$ [514] state at 6.2 keV and the $7/2^+$ [404] ground state of Ta-181.

IV. SOLID-STATE APPLICATIONS

Considering the range of isomer shifts that have been observed with the 6.2-keV gamma resonance it is obvious that its sensitivity to small changes in $|\psi_0|^2$ should be quite unique. The value of $\Delta \langle r^2 \rangle$ derived in the preceding section allows a direct comparison of its sensitivity with that of the 14.4-keV gamma resonance of Fe-57. We find that comparable changes in the solid-state environment, for example equal changes in the population of Ta-6s and Fe-4s orbitals, shift the transition energy in units of the respective natural linewidths by amounts on the order of 4000 to 1 for Ta-181 and Fe-57, respectively. The magnitude of this ratio illustrates one of the causes of the considerable line broadening observed in Ta-181 resonance lines. Taking into account the present experimental linewidths the resolution with Ta-181 isomer shifts is by a factor of about 400 higher than in the Fe-57 case. This unique resolving power is especially attractive for solid-state applications. To illustrate this possibility we would like to discuss the influence of temperature and hydrostatic pressure on the transition energy.

A. Temperature Dependence of the Transition Energy

The effects of temperature on the energy of Mössbauer gamma rays have been studied up to now in detail only for Fe-57 [39-42] and Sn-119 [43]. In both cases the observed temperature shifts were found to be predominantly caused by the second-order

Doppler (SOD) effect (thermal redshift) [44] .

In contrast to this, we have found that the
energy of the 6.2-keV gamma rays, emitted from
Ta-181 as a dilute impurity in transition metals,
exhibits a strong temperature dependence far beyond
the SOD shift [19] . Depending on the host metals,
the observed temperature shifts vary from -32 to
+8 times the thermal redshift expected for a Debye
solid in the classical high-temperature limit. These
large temperature shifts are mainly caused by tem-
perature induced changes of $|\psi_o|^2$, since both the
energy of the 6.2-keV gamma rays is extremely sen-
sitive to small changes in $|\psi_o|^2$, and the SOD effect
is expected to be quite small due to the large nuc-
lear mass of Ta-181 and the low gamma ray transition
energy.

The present experiments were performed on sour-
ces which were heated in vacuum from room tempera-
ture up to ~ 1000 K. The single-line Ta metal ab-
sorber was kept at room temperature.

The experimental results for five of the stud-
ied sources are shown in Fig. 7, where the line
shifts relative to a Ta metal absorber are plotted
versus the source temperatures. For comparison the
SOD shift, expected for a Debye solid in the limit
of high temperatures, is also plotted. All curves
are drawn on the same scale. The solid lines are
the results of least-squares fits of straight lines
to the data.

It is striking that in the case of the nickel
host the transition energy increases with tempera-
ture with a slope which is 32 times larger and of
opposite sign than the one expected from the SOD
shift alone. It represents a lineshift of 2.3 natur-
al widths per degree. On the other hand the slopes
of the temperature shifts for W, Ta, and Pt hosts
have the same sign as the SOD shift, but are up to
8 times larger.

We may write the experimentally observed tem-
perature variation of the line position S as

$$\left(\frac{\partial S}{\partial T}\right)_P = \left(\frac{\partial S_{SOD}}{\partial T}\right)_P + \left(\frac{\partial S_{IS}}{\partial T}\right)_V + \left(\frac{\partial S_{IS}}{\partial \ell nV}\right)_T \left(\frac{\partial \ell nV}{\partial T}\right)_P (3)$$

The first term accounts for the temperature variation of the SOD shift, which is given for a Debye solid in the limit of high temperatures by $-3k/2Mc$ in velocity units and amounts to $-2.30 \cdot 10^{-4}$ mm/s per degree for the present gamma ray transition. The second term represents the explicit temperature dependence of the isomer shift at constant volume due to temperature induced changes of the total electron density at the nucleus. The third term describes the volume dependence of the isomer shift caused by thermal expansion of the lattice.
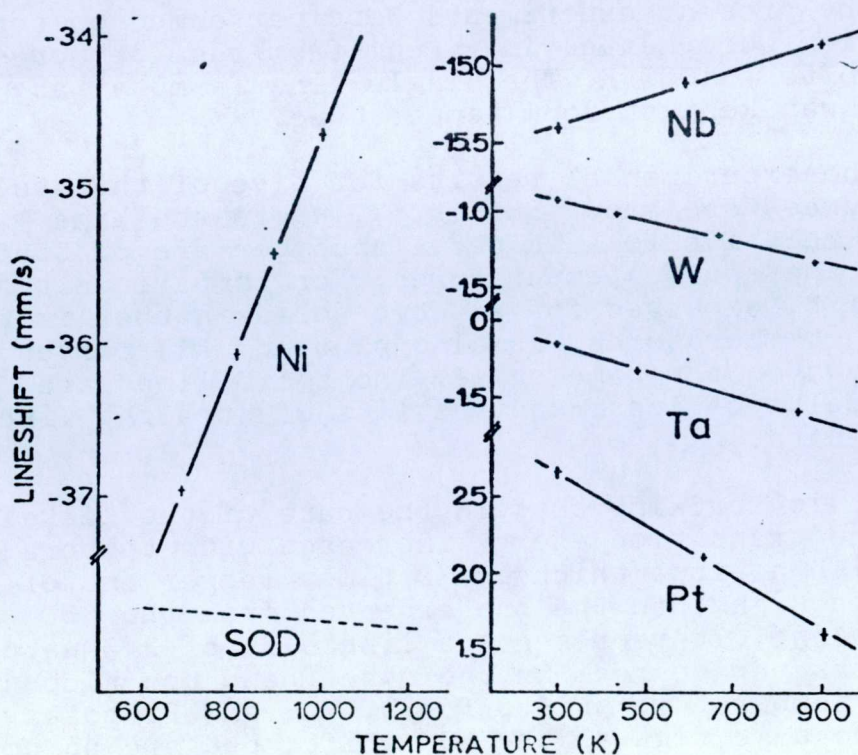

Fig. 7. Temperature dependence of line positions for sources of W-181 diffused into Ni, Nb, W, Ta, and Pt host metals.

The volume dependent part of the temperature shift, represented by the third term in Eqn. 3, should be positive in all cases since $(\partial|\psi_o|^2/\partial\ell nV)_T$ is expected to be negative. In order to explain the large negative temperature shifts observed for the Pt, Pd, Ir, W, and Ta hosts we have to postulate therefore a negative sign for the second term, at least in these cases. This would correspond to an explicit increase of $|\psi_o|^2$ with temperature.

Table 4 summarizes the temperature shift data, with the experimental results for the isobaric temperature variation of the transition energy, $(\partial S/\partial T)_p$, presented in column 2. The values for the isobaric temperature dependence of the isomer shift, $(\partial S_{IS}/\partial T)_p$, were derived by subtracting the contribution due to SOD effect from $(\partial S/\partial T)_p$. In view of

Table 4. Summary of experimental results and derived quantities for dilute impurities of Ta-181 in transition metal hosts.

host metal	$(\partial S/\partial T)_P$ $(10^{-4}$ mm/s/deg.)	$(\partial S_{IS}/\partial T)_P$ $(10^{-4}$ mm/s/deg.)	$(\partial\ell nV/\partial T)_P$ $(10^{-5}$ deg.$^{-1})$
Ni	73.2 (35)	75.5 (35)	5.2
Nb	9.2 (10)	11.5 (10)	2.5
Mo	3.6 (6)	5.9 (5)	1.7
Pd	-16.7 (70)	-14.4 (70)	3.5
Ta	-8.0 (5)	-5.7 (5)	2.0
W	-7.1 (2)	-4.8 (2)	1.4
Ir	-10.7 (33)	-8.4 (33)	2.0
Pt	-17.6 (9)	-15.3 (9)	2.9

the fact that these corrections are small compared to the total temperature shifts, and that the measurements were carried out in the temperature range 300 to 1000 K, where the high temperature Debye model should approximately hold, this procedure should be satisfactory within the present accuracy. Also presented are representative values for the thermal expansion coefficients of the host metals (column 4), averaged over the temperature regions of the present experiments.

Until now temperature shifts of the 6.2-keV gamma rays have been reported only for a tungsten host by Taylor et al. [45], and their results agree well with the present measurements. In the case of Fe-57 temperature shifts of the energy of the 14.4-keV gamma rays have been measured for iron metal [41] and for dilute impurities of Fe-57 in 3d, 4d, and 5d transition metals [42]. Even though these shifts arise mainly from the SOD effect, the derived values for $(\partial S_{IS}/\partial T)_p$ exhibit characteristics similar to the present case [46].

A separation of $(\partial S_{IS}/\partial T)_p$ into an explicitly temperature dependent part and a volume dependent part can be accomplished only with additional information on the volume dependence of the isomer shift. This can be obtained from the results of high-pressure experiments.

B. Pressure Dependence of the Transition Energy

The experimental technique for high-pressure experiments with the 6.2-keV gamma resonance has to cope with problems arising mainly from the low gamma ray transition energy and the high sensitivity of the resonance line. It was already observed by Sauer [4] that small lattice distortions can broaden the Mössbauer line appreciably.

A schematic of the high-pressure setup developed for the Ta-181 experiments is given in Fig. 8. The source is immersed in a pressurized oil bath to insure hydrostatic pressure. The 2 mm thick beryl-

lium metal window limits the applied pressures to approximately 5 kbar.
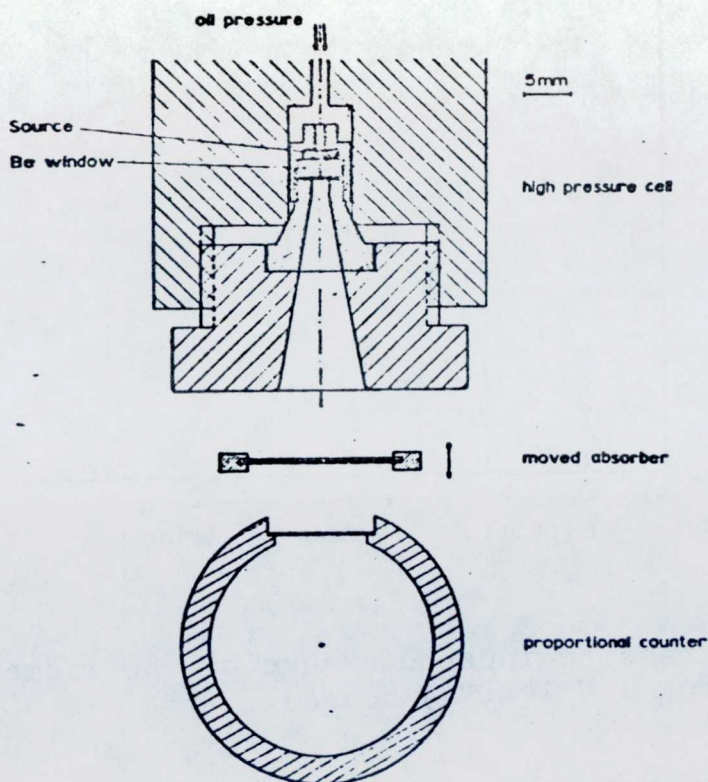

Fig. 8. Schematic of the experimental setup for high-pressure experiments.

Up to now we have performed pressure experiments with sources diffused into tungsten and tantalum metal. The results for a tantalum metal source are presented in Fig. 9, where the change in line position is plotted versus the applied hydrostatic pressure. As expected, the transition energy decreases with increasing pressure, in agreement with a negative sign for $\Delta <r^2>$, assuming a simple scaling of $|\psi_0|^2$ with volume. The observed lineshift corresponds to ~ 11 times twice the natural width

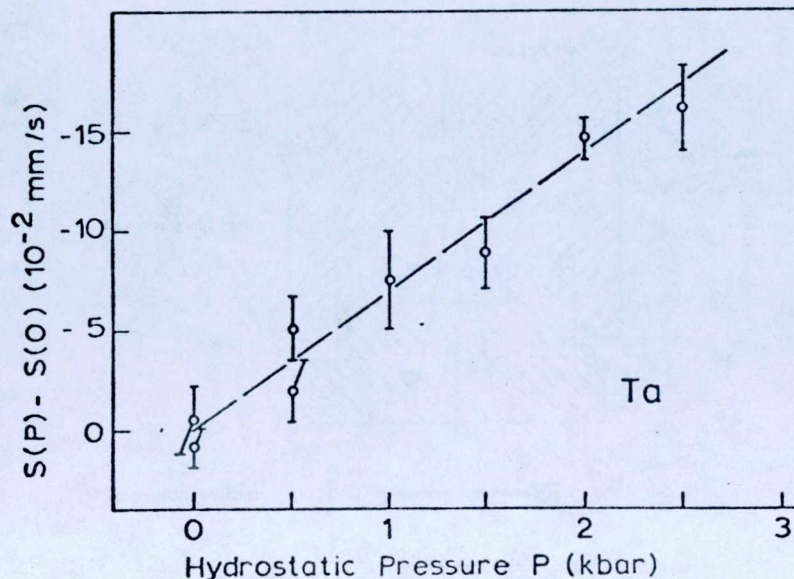per kbar, or approximately one experimental line-
width per 3 kbar.

Fig. 9. Pressure induced change of the isomer shift
for a W-181(Ta) source.

The pressure shift results for tungsten and tan-
talum metal hosts are summarized in Table 5. The
isothermal pressure shifts, $(\partial S/\partial P)_T$, were obtained
by fitting straight lines to the data. The contri-
bution to $(\partial S/\partial P)_T$, caused by a pressure dependence
of the SOD effect [40], is expected to be negligib-
le in the present case. We may then interpret the
experimental pressure shifts as arising entirely from
a pressure-induced variation of $|\psi_o|^2$. In the last
column of Table 5 derived values for the isothermal
volume dependence of the isomer shift are listed, ob-
tained by dividing $(\partial S/\partial P)_T$ by the compressibilities
given in column 3 [47, 48].

Table 5. Summary of pressure shift results for tantalum and tungsten metal hosts.

host metal	$(\frac{\partial S}{\partial P})_T$ $(10^{-2}$ mm/s/kbar)	$(\frac{\partial \ln V}{\partial P})_T$ $(10^{-4}$ kbar$^{-1})$	$(\frac{\partial S_{IS}}{\partial \ln V})_T$ (mm/s)
Ta	-6.9 (7)	-5.10	135 (14)
W	-4.8 (9)	-3.16	152 (30)

C. Explicit Temperature Dependence of the Isomer Shift.

The results for $(\partial S_{IS}/\partial \ln V)_T$ can be used for a quantitative analysis of the temperature dependence of the isomer shift in the cases of tungsten and tantalum metal hosts. A summary of the analysis is given in Table 6. With the known thermal expansion coefficients of Ta and W metal (Table 4) we are in a position to calculate the volume dependent part of $(\partial S_{IS}/\partial T)_P$, using our results for $(\partial S_{IS}/\partial \ln V)_T$. The results, presented in column 2 of Table 6, are of opposite sign than the experimental values for the total isobaric temperature dependence of S_{IS} (Table 4, column 3).The differences of both are interpreted as the explicitly temperature dependent part of $(\partial S_{IS}/\partial T)$. The final results are given in column 3. In both cases, the transition energy decreases explicitly with increasing temperature by approximately equal amounts.

Taking $\Delta \langle r^2 \rangle = -5 \cdot 10^{-2}$ fm^2, this decrease in transition energy corresponds to an increase in $|\psi_0|^2$ by amounts of $6.2 \cdot 10^{21}$ cm^{-3} per degree and of $4.9 \cdot 10^{21}$ cm^{-3} per degree for the tantalum and tungsten hosts, respectively. This increase in $|\psi_0|^2$ can be interpreted as an effective d→s electron transfer with increasing temperature at constant volume. Using the results of relativistic

Table 6. Analysis of temperature shifts for tantalum and tungsten metal.

host metal	$(\partial S_{IS}/\partial \ell n V)_T (\partial \ell n V/\partial T)_P$ $(10^{-4}$ mm/s/deg.)	$(\frac{\partial S_{IS}}{\partial T})$ $(10^{-4}$ mm/s/deg.)
Ta	27 (3)	-33 (4)
W	21 (5)	-26 (5)

Dirac-Fock calculations for free-ion configurations of tantalum [33], we find that our results for the explicit increase in $|\psi_0|^2$ with increasing temperature correspond to a transfer of approximately 10^{-5} electrons per degree to the s band.

An explicit temperature dependence of $|\psi_0|^2$ has been postulated before for β-tin [43] as well as for iron metal and dilute impurities of iron in transition metal hosts [46]. In both cases $|\psi_0|^2$ was found to increase explicitly with temperature by amounts corresponding to an increasing population of s states by approximately 10^{-5} electrons per degree, as in the present case.

Similar effects have been discussed theoretically in connection with the temperature dependence of the Knight shift, and have been interpreted by Kasovski and Falicov [49] as arising from an effective decrease in the strength of the lattice potential with increasing temperature, caused by thermal vibrations. In this way the energy bands become more free-electron like with increasing temperature, leading to an increase in the s character of the wave functions and accordingly to an increase in $|\psi_0|^2$. It is expected that these effects would exhibit a strong dependence on the electronic structures of the host metals. An extension of the study of pressure shifts to other host metals, especially

to those for which temperature shifts have already been measured, is therefore of considerable interest.

ACKNOWLEDGEMENTS

REFERENCES

1. H. de Waard and G. J. Perlow, Phys. Rev. Letters 24, 566 (1970).
2. W. A. Steyert, R. D. Taylor, and E. K. Storms, Phys. Rev. Letters 14, 739 (1965).
3. C. Sauer, E. Matthias, and R. L. Mössbauer, Phys. Rev. Letters 21, 961 (1968).
4. C. Sauer, Z. Physik 222, 439 (1969); and references therein.
5. G. Kaindl and D. Salomon, Perspectives in Mössbauer Effect Spectroscopy, S. G. Cohen and M. Pasternak, eds., Plenum Press, New York (1973), in print.
6. G. Kaindl and D. Salomon, University of California, Lawrence Berkeley Laboratory Report UCRL-20426, 215 (1970).
7. G. Kaindl and D. Salomon, Phys. Letters 42A, 333 (1973).
8. G. Kaindl, D. Salomon, and G. Wortmann, Phys. Rev. Letters 28, 952 (1972).
9. G. Kaindl and D. Salomon, Phys. Letters 40A, 179 (1972).
10. G. Kaindl and D. Salomon, Bull. Am. Phys. Soc. 17, 681 (1972).

11. G. Wortmann, Phys. Letters 35A, 391 (1971).
12. G. Kaindl, D. Salomon, and G. Wortmann, submitted to Phys. Rev. B.
13. G. Kaindl, M. R. Maier, H. Schaller, and F. Wagner, Nucl. Instr. Methods 66, 277 (1968).
14. G. Wortmann, PhD Thesis, Technische Universität München (1971).
15. D. Salomon, PhD Thesis, Lawrence Berkeley Laboratory Report LBL-1276 (1972).
16. G. T. Trammel and J. P. Hannon, Phys. Rev. 180, 337 (1969).
17. Yu. M. Kagan, A. M. Afanasev, and V. K. Vojtovetskii, Soviet Physics JETP Letters 9, 91 (1969).
18. G. Kaindl and D. Salomon, Phys. Letters 32B, 364 (1970).
19. G. Kaindl and D. Salomon, submitted to Phys. Rev. Letters.
20. R. D. Taylor and E. K. Storms, Bull. Am. Phys. Soc. 14, 836 (1969).
21. S. M. Quaim, Proc. Phys. Soc. (London) 90, 1065 (1967).
22. G. Wortmann, unpublished results (1973).
23. B. Window, G. Longworth, and C. E. Johnson, J. Phys. C: Solid St. Phys. 3, 2156 (1970).
24. A. H. Muir, Jr., K. J. Ando, and H. M. Coogan, Mössbauer Effect Data Index 1958-1965, Interscience Publsihers, New York (1966).
25. G. Kaindl and D. Salomon, Proc. International Conference on Applications of the Mössbauer Effect, Israel (1972).
26. G. Wortmann, F. E. Wagner, and G. M. Kalvius, Proc. International Conference on Applications of the Mössbauer Effect, Israel (1972).
27. G. Wortmann, F. E. Wagner, and G. M. Kalvius, Phys. Letters 42A, 483 (1973).
28. G. K. Shenoy and G. M. Kalvius, Hyperfine Interactions in Excited Nuclei, G. Goldring and R. Kalish, eds., Gordon and Breach, New York (1971), p. 1201.
29. X. A. da Silva, A. A. Gomes, and J. Danon, Phys. Rev. B4, 1161 (1971).
30. C. G. Gelatt and H. Ehrenreich, Bull. Am. Phys. Soc. 18, 93 (1973).
31. S. L. Ruby and G. K. Shenoy, Phys. Rev. 186, 326 (1969).

32. G. Kaindl, D. Kucheida, W. Potzel, F. E. Wagner, U. Zahn, and R. L. Mössbauer, _Hyperfine Interactions in Excited Nuclei_, G. Goldring and R. Kalish, eds., Gordon and Breach, New York (1971), p. 595.

33. J. B. Mann, Los Alamos Scientific Laboratory, University of California, private communication (1970 - 1972).

34. J. Blomquist, B. Ross, and M. Sundbom, J. Chem. Phys. 55, 141 (1971).

35. L. W. Panek and G. J. Perlow, Argonne National Laboratory Report ANL-7631 (1969).

36. L. D. Roberts, D. O. Patterson, J. O. Thomson, and R. P. Levey, Phys. Rev. 179, 656 (1969).

37. W. Potzel, F. E. Wagner, R. L. Mössbauer, G. Kaindl, and H. E. Seltzer, Z. Physik 241, 179 (1971).

38. H. Micklitz and P. H. Barrett, Phys. Rev. Letters 28, 1547 (1972).

39. R. V. Pound and G. A. Rebka, Jr., Phys. Rev. Letters 4, 274 (1960).

40. R. V. Pound, G. B. Benedek, and R. Drever, Phys. Rev. Letters 7, 405 (1961).

41. R. S. Preston, S. S. Hanna, and J. Heberle, Phys. Rev. 128, 2207 (1962).

42. W. A. Steyert and R. D. Taylor, Phys. Rev. 134, A716 (1964).

43. G. M. Rothberg, S. Guimard, and N. Benczer-Koller, Phys. Rev. B1, 136 (1970).

44. B. D. Josephson, Phys. Rev. Letters 4, 341 (1960).

45. R. D. Taylor and E. K. Storms, Bull. Am. Phys. Soc. 14, 836 (1969).

46. R. M. Housley and F. Hess, Phys. Rev. 164, 340 (1967).

47. D. I. Bolef, J. Appl. Phys. 32, 100 (1961).

48. F. H. Featherston and J. R. Neighbours, Phys. Rev. 130, 1324 (1963).

49. R. V. Kasovski and L. M. Falicov, Phys. Rev. Letters 22, 1001 (1969).